

5-1-2009

# Assessing access of galactic cosmic rays at Moon's orbit

Chia-Lin L. Huang  
hcl@guero.sr.unh.edu

Harlan E. Spence  
*Boston University*, harlan.spence@unh.edu

B. T. Kress

Follow this and additional works at: [https://scholars.unh.edu/physics\\_facpub](https://scholars.unh.edu/physics_facpub)



Part of the [Physics Commons](#)

---

## Recommended Citation

Huang, C.-L., H. E. Spence, and B. T. Kress (2009), Assessing access of galactic cosmic rays at Moon's orbit, *Geophys. Res. Lett.*, 36, L09109, doi:10.1029/2009GL037916.

This Article is brought to you for free and open access by the Physics at University of New Hampshire Scholars' Repository. It has been accepted for inclusion in Physics Scholarship by an authorized administrator of University of New Hampshire Scholars' Repository. For more information, please contact [nicole.hentz@unh.edu](mailto:nicole.hentz@unh.edu).

---

# Assessing access of galactic cosmic rays at Moon's orbit

## **Rights**

Copyright 2009 by the American Geophysical Union.

## Assessing access of galactic cosmic rays at Moon's orbit

Chia-Lin Huang,<sup>1</sup> Harlan E. Spence,<sup>1</sup> and Brian T. Kress<sup>2</sup>

Received 25 February 2009; revised 3 April 2009; accepted 15 April 2009; published 15 May 2009.

[1] Characterizing the lunar radiation environment is essential for preparing future robotic and human explorations on lunar bases. Galactic cosmic rays (GCR) represent one source of ionizing radiation at the Moon that poses a biological risk. Because GCR are charged particles, their paths are affected by the magnetic fields along their trajectories. Unlike the Earth, the Moon has no strong, shielding magnetic field of its own. However, as it orbits Earth, the Moon traverses not only the weak interplanetary magnetic field but also the distant magnetic tail of Earth's magnetosphere. We combine an empirical magnetic field model of Earth's magnetosphere with a fully-relativistic charged particle trajectory code to model and assess the access of GCR at the Moon's orbit. We follow protons with energies of 1, 10 and 100 MeV starting from an isotropic distribution at large distances outside a volume of space including Earth's magnetosphere and the lunar orbit. The simulation result shows that Earth's magnetosphere does not measurably modify protons of energy greater than 1 MeV at distances outside the geomagnetic cutoff imposed by Earth's strong dipole field very near to the planet. Therefore, in contrast to Winglee and Harnett (2007), we conclude that Earth's magnetosphere does not provide any substantial magnetic shielding at the Moon's orbit. These simulation results will be compared to LRO/CRaTER data after its planned launch in June 2009. **Citation:** Huang, C.-L., H. E. Spence, and B. T. Kress (2009), Assessing access of galactic cosmic rays at Moon's orbit, *Geophys. Res. Lett.*, *36*, L09109, doi:10.1029/2009GL037916.

### 1. Introduction

[2] High-energy protons, such as galactic cosmic rays (GCR) with energies sufficient to penetrate spacecraft shielding or a spacesuit, have undesirable biological effects on astronauts as well as effects on electronic systems. An energetic charged particle's path is affected by local magnetic fields along its trajectory. The Moon spends  $\sim 15\%$  of its orbit in the Earth's magnetosphere (a fraction computed using a magnetopause location based on Shue *et al.* [1998]) and the rest in the interplanetary medium. Therefore, it is relevant to consider whether GCR access to the Moon is influenced by the GCR's passage through the magnetotail as opposed to in the interplanetary medium.

[3] When particles are going through regions of different magnetic strength and direction, their path will be bent and

deflected due to the Lorentz force. Because of their larger gyroradii, high-energy particles are less influenced by the geomagnetic field and its gradients than are low-energy particles. The Earth's strong dipole field usually shields the inner magnetosphere from direct penetration of energetic particles by magnetically deflecting the particles away from the Earth [Störmer, 1955; Smart and Shea, 1994; Smart *et al.*, 2000, and references therein]. The degree of geomagnetic shielding is quantified in terms of geomagnetic cutoffs [Störmer, 1955]. The radial boundary of such a forbidden region for particle penetration is defined by the equation:

$$r = \sqrt{\frac{Mq}{pc}} \frac{\cos^2 \lambda}{1 + \sqrt{1 + \cos^3 \lambda}} \quad (1)$$

where  $M$  is the dipole moment,  $q$  and  $p$  are particle charge and momentum,  $\lambda$  is the latitude and  $r$  is the radial distance from the center of the dipole field. The cutoff distance of 1, 10, and 100 MeV protons in Earth's dipole field are at 15.4, 8.6, and 4.8  $R_E$  in the equatorial plane, respectively. In this simple dipole approximation, outside their geomagnetic cutoffs and according to their energy, the distribution of GCR particles should be essentially unmodified from that of the interplanetary medium (i.e., isotropic) [Jokipii and Kóta, 2000]. For example, according to observations by the SAMPEX satellite, the energetic proton flux with energy  $\geq 9$  MeV is nearly constant at all  $L$  shells (radial distance of trapped energetic particles in Earth radii) outside the cutoff distance at  $L \sim 4$  during time intervals without a solar energetic proton event (J. B. Blake, private communication, 2008). Thus, the simple dipole approximation and Störmer theory seems to explain well GCR observations relatively close to Earth.

[4] On the other hand, a recent numerical study by Winglee and Harnett [2007] concluded that the quiet-time magnetosphere could offer some magnetic shielding from GCR and SEP at the Moon's orbit. Winglee and Harnett [2007] argued that GCR will be shielded by the magnetosphere since a GCR's gyroradius is comparable to the length scale of the magnetotail. By integrating the magnetic intensity from distant points to the Moon in a global MHD code, they reported that Earth's magnetosphere could shield particles up to 5 GeV/nucleon at the Moon's orbit, especially at an equatorial lunar base facing the Earth. Their result appears at odds with simple Störmer theory and SAMPEX observations. To reassess the magnetosphere's role in magnetic shielding of GCR at the Moon's orbit, we follow the trajectories of GCR particles using a fully-relativistic particle tracing code and an empirical magnetospheric model. Based on the simulation results, we resolve the spatial variations of particle access at lunar orbit to identify possible interplanetary modulation sources and to

<sup>1</sup>Center for Space Physics, Boston University, Boston, Massachusetts, USA.

<sup>2</sup>Department of Physics and Astronomy, Dartmouth College, Hanover, New Hampshire, USA.

### GCR simulation domain at Moon's orbit: $100 R_E$ sphere

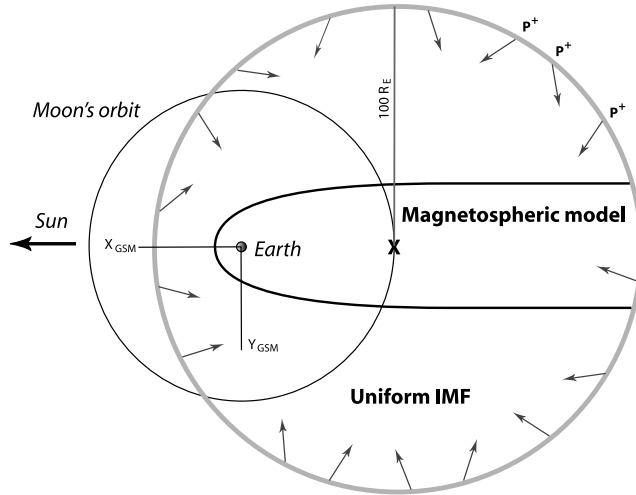


**Figure 1.** Illustration of GCR particle simulation domain with respect to the Moon's orbit. Protons are launched isotropically from a  $100 R_E$  sphere and proton trajectories are calculated in realistic magnetospheric fields.

determine the extent of magnetospheric shielding at the Moon.

## 2. Computational Method

[5] We simulate proton trajectories to model the access of high-energy particles at the Moon's orbit using a global magnetospheric model and a particle tracing code. As shown in Figure 1, test particles at fixed energies are launched isotropically from a spherical shell of radius  $100 R_E$  centered on  $X = -60 R_E$  in Geocentric Solar Magnetospheric (GSM) coordinates, i.e., the deepest lunar location in the magnetotail. Isotropic spatial and velocity distributions are reasonable assumptions for GCR particles outside but near Earth's magnetosphere [Jokipii and Kóta, 2000]. If there is any geomagnetic shielding of the high-energy particles in this  $100 R_E$  sphere, the simulated particle flux will be lower in regions where magnetic shielding is significant.

[6] The time-dependent, three-dimensional magnetic configuration of Earth's outer magnetotail is not well-known, because of the lack of large-scale in-situ measurements, especially at the Moon's orbit. However, its statistical average properties are reasonably understood and are relevant for our use [Spence et al., 1989]. In this study, we use an empirical magnetic field model, Tsyganenko 1996 (noted as T96) [Tsyganenko, 1995, 1996], as the magnetospheric model. T96 is the latest empirical magnetospheric model that simulates Earth's magnetotail beyond  $-15 R_E$  tailward, and has been shown to make reasonable predictions in the inner magnetosphere during intervals of quiet and moderate activities [Huang et al., 2008]. We calculate the model fields with typical and time-invariant solar wind and interplanetary magnetic field (IMF) conditions (input parameters are:  $P_{D_{\text{dyn}}} = 2$  nPa, IMF  $B_X = B_Y = 0$  nT, IMF  $B_Z = +5$  nT,  $D_{\text{st}} = -5$  nT), all well

within the valid input range of the model. To facilitate comparison with their results, we use the same the IMF conditions as those used by Winglee and Harnett [2007] for the stronger magnetic field strength event in their study. Outside the model magnetopause boundary [Shue et al., 1998], we use the same magnetic field intensity and direction, to represent the interplanetary magnetic field.

[7] Figure 2 shows the magnetic field magnitude of the magnetosphere used in our study in the equatorial (Figure 2, top) and noon-midnight (Figure 2, bottom) planes. The total field intensity is shown with color in a logarithmic scale. The grey curve indicates the location of the magnetopause and the white X marks the deepest lunar location in the magnetotail. The field intensity is highest near the Earth where the internal dipolar field dominates. In the pressure-balanced magnetotail region ( $X < -10 R_E$ ), the low-beta lobe field has stronger magnetic fields than the high-beta plasmasheet field.

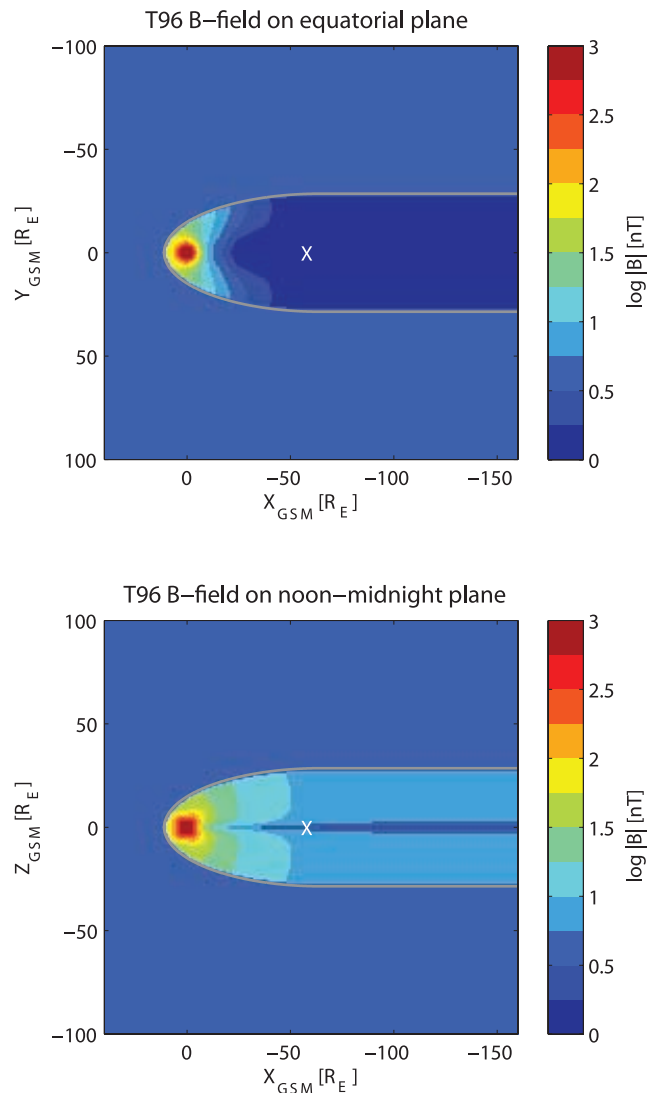


**Figure 2.** Magnetic field strength of the magnetosphere at the (top) equatorial and (bottom) noon-midnight planes based on Tsyganenko 1996 model during typical solar wind and IMF conditions.

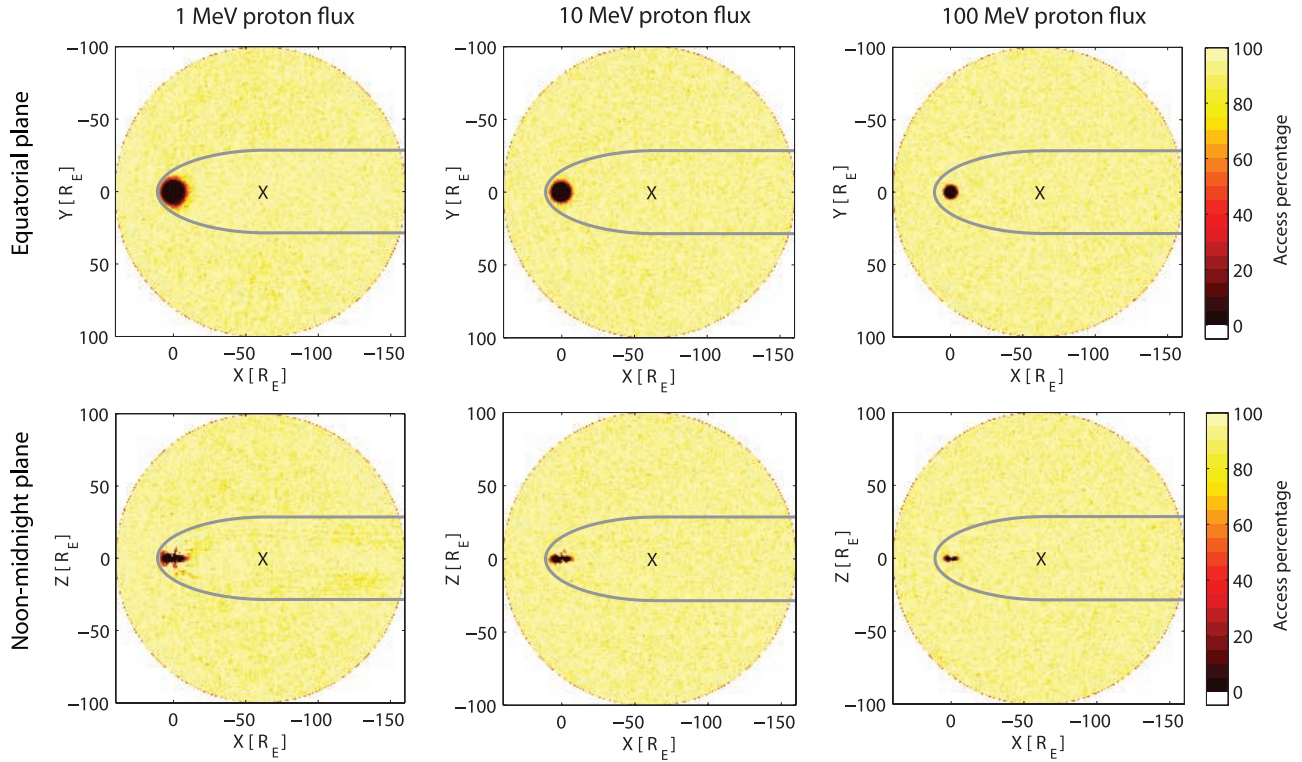


**Figure 3.** Proton access percentage on the (top) equatorial and (bottom) noon-midnight planes from test particle simulations for different proton energies of 1, 10 and 100 MeV. 100% means the region is unshielded; 0% means the region is fully shielded.

[8] The fully-relativistic particle tracing code solves a charged particle’s equation of motion using a 4th order Runge-Kutta integrator with the step size adjusted to be 1% of the instantaneous gyro-period of the particle [Kress *et al.*, 2004]. The time-independent magnetic field is calculated from the T96 model along each particle’s trajectory. Electric fields are assumed to be zero for simplicity; their contribution is negligible to energetic particles with GCR energies. We launch test particles isotropically from the  $100 R_E$  spherical shell as shown in Figure 1. As a result, everywhere within the sphere should have uniform particles in all directions in the limit where no magnetic fields are present inside the sphere. We follow protons (the major composition of GCR) with energies of 1, 10, and 100 MeV. This range includes the threshold energy above which is of biological interest ( $\geq 10$  MeV) [Wilson *et al.*, 1997], along with factors of 10 lower and higher. At 1 MeV, a proton can only penetrate  $\sim \mu\text{m}$  in aluminum, and so is easily shielded [Cucinotta and Durante, 2006], but is included as a lower bracket to primary energies of interest.

[9] We follow particle trajectories for 20 simulated minutes, a time required so that the simulated proton flux reaches a quasi-steady state throughout the spatial volume. For each energy, we launch 20 million particles uniformly distributed on the spherical shell with isotropic spatial and directional distributions. Once a particle leaves the outer domain, it is terminated. We calculate the simulated particle flux by counting the number of particle crossings through the equatorial and noon-midnight planes. To estimate the proton access rate, we normalize the simulated flux by the

expected flux of a cut plane when no magnetic field is present in the sphere. Then we compare particle access percentage in different regions of space, e.g., in the interplanetary medium and magnetosphere to determine the extent of magnetospheric shielding to different energy protons at the Moon’s orbit.

### 3. Simulation Results

[10] Figure 3 shows the access percentage of simulated protons on the equatorial (Figure 3, top) and noon-midnight (Figure 3, bottom) planes for protons with energies of 1, 10, and 100 MeV (from left to right plots, respectively). Each plot is colored by the access percentage with the same color bar. The grey curve indicates the location of the model magnetopause and the black  $X$  at  $X_{GSM} = -60 R_E$  denotes the deepest lunar location in the magnetotail.

[11] The proton access percentage in the magnetosphere and those in the interplanetary medium at the Moon’s orbit are very high and similar for both cut planes and for all particle energies. The difference between the averaged access rates inside and outside of the magnetosphere at the Moon’s orbit on the equatorial plane is less than 1.8% for all particle energies. Hence, there is no significant magnetotail shielding for protons with energy greater than 1 MeV at the Moon’s orbit according to our simulation.

[12] One clear difference between all energy panels is the distance where access rates drop sharply in the near-Earth region, i.e., the geomagnetic cutoffs. The cutoff distance at each particle energy is estimated to be where the particle

flux decreases to 10% of the average flux outside the forbidden region. For 1, 10 and 100 MeV protons, the cutoff distances are at 7.8, 6.4, and 4.1  $R_E$ , respectively. Comparing to the cutoff distances based on Störmer theory, our values are smaller and the shape of the forbidden regions is asymmetric, especially for the low-energy protons. This is due to the solar wind-distorted Earth's dipole field which forms an asymmetric magnetosphere with compressed field on the dayside and elongated on the nightside. Consequently, the cutoff locations of GCR are expected to be highly dependent on the specific magnetic field model that is incorporated in the particle trajectory calculations [Smart et al., 2000]. Nevertheless, the cutoff distances predicted in our calculations are similar to those calculated earlier from Störmer theory in a simple dipole.

#### 4. Conclusions

[13] To determine any variation of GCR flux due to possible magnetotail shielding at the Moon's orbit, we performed particle simulations using realistic magnetic fields to model the lunar radiation environment. Time reversed trajectories have been used traditionally to locate geomagnetic cutoffs by launching particles from a hypothetical detection point and tracking the time-reversed path back through a model magnetic field [Smart and Shea, 1994; Smart et al., 2000]. Using this method, Smart et al. [2000] predicted the cutoff rigidity of GCR particles when comparing to ground observations. In contrast to the time reversed trajectories method, we launched millions of test protons into a 100  $R_E$  spherical shell centered at the deepest lunar location in the magnetotail and calculate the particle flux within the simulation domain. If there is any geomagnetic shielding of energetic particles, the simulated proton flux will be lower in regions where the shielding effect is significant. As shown in Figure 3, the difference between the proton access percentage inside and outside of the magnetosphere is insignificant (except inside geostationary orbit, consistent with complimentary technique used by Smart and Shea [1994]) at the Moon's orbit (<2%, which is comparable to the statistical variance of our estimates). These simulation results confirm that Earth's magnetosphere does not substantially modify GCR (with proton energies greater than 1 MeV) at the lunar environment during typical solar wind conditions.

[14] Following Störmer's [1955] work, an argument using Liouville's theorem may be used to show that at rigidities above the cutoff, the directional flux of particles is equivalent to that outside the influence of the geomagnetic field [Lemaitre and Vallarta, 1933; Swann, 1933]. Our simulation confirmed that the proton flux outside the forbidden regions are nearly constant in a realistic magnetosphere, as shown in Figure 3. As noted earlier, Winglee and Harnett [2007] reached a different conclusion about magnetotail shielding on GCR particles at the Moon's orbit. Their conclusion may be the result of overly simple assumptions, such as assuming that a particle's path is a straight line and using magnetic deflection as a proxy for magnetic shielding. First, the assumption that a particle's path is straight line is inappropriate; for instance, the gyro-radius

of 1, 10 and 100 MeV protons in the magnetotail lobe field ( $B = 20$  nT) is 1.3, 3.7, and 10.6  $R_E$ , respectively (i.e., a small fraction of the entire magnetotail). Second, magnetic deflection is not the same as magnetic shielding. Particles can be deflected both away from or toward the Moon when going through different regions of magnetic intensity, so net directionality is important. In contrast to Winglee and Harnett [2007], our particle simulations demonstrate that the Earth's magnetosphere does not have sufficient magnetic field intensity to shield effectively GCR protons from the lunar environment (or indeed anywhere beyond their geomagnetic cutoffs in Earth's inner magnetosphere).

[15] This work provides important information about the lunar environment for the future planning of lunar landings and exploration. At present, there are limited observations of GCR at the Moon's orbit to measure directly the energy-dependent access of GCR to the Moon throughout its orbit, including in the magnetotail. In the near future, the Cosmic Ray Telescope for the Effects of Radiation (CRaTER) on board of NASA Lunar Reconnaissance Orbiter mission (LRO) [Chin et al., 2007; H. E. Spence et al., CRaTER: The Cosmic Ray Telescope for the Effects of Radiation experiment on the Lunar Reconnaissance Orbiter mission, submitted to Space Science Reviews, 2009] will measure GCR fluxes above 10 MeV. We plan to compare our simulation results with measurements collected by CRaTER after its launch in June 2009 to quantify directly the access of GCR at the Moon's orbit under the influence of Earth's magnetosphere.

[16] **Acknowledgments.** We thank Tony Case, Mary Hudson, Andrew Jordan and Simon Shepherd for useful discussions and suggestions. We greatly appreciate support from LRO/CRaTER project under contract NASA NNG05EB92C.

#### References

- Chin, G., et al. (2007), Lunar reconnaissance orbiter overview: The instrument suite and mission, *Space Sci. Rev.*, 129, 391–419.
- Cucinotta, F. A., and M. Durante (2006), Cancer risk from exposure to galactic cosmic rays: Implications for space exploration by human beings, *Lancet Oncol.*, 7, 431–435.
- Huang, C.-L., H. E. Spence, H. J. Singer, and N. A. Tsyganenko (2008), A quantitative assessment of empirical magnetic field models at geosynchronous orbit during magnetic storms, *J. Geophys. Res.*, 113, A04208, doi:10.1029/2007JA012623.
- Jokipii, J. R., and J. Kóta (2000), Galactic and anomalous cosmic rays in the heliosphere, *Astrophys. Space Sci.*, 274, 77–96.
- Kress, B. T., M. K. Hudson, K. L. Perry, and P. L. Slocum (2004), Dynamic modeling of geomagnetic cutoff for the 23–24 November 2001 solar energetic particle event, *Geophys. Res. Lett.*, 31, L04808, doi:10.1029/2003GL018599.
- Lemaitre, G., and M. S. Vallarta (1933), On Compton's latitude effect of cosmic radiation, *Phys. Rev.*, 43, 87–91.
- Shue, J.-H., et al. (1998), Magnetopause location under extreme solar wind conditions, *J. Geophys. Res.*, 103, 17,691–17,700.
- Smart, D. F., and M. A. Shea (1994), Geomagnetic cutoffs for space dosimetry applications, *Adv. Space Res.*, 14, 787–797.
- Smart, D. F., M. A. Shea, and E. O. Flückiger (2000), Magnetospheric models and trajectory calculations, *Space Sci. Rev.*, 93, 305–333.
- Spence, H., M. Kivelson, R. Walker, and D. McComas (1989), Magnetospheric plasma pressures in the midnight meridian: Observations from 2.5 to 35  $R_E$ , *J. Geophys. Res.*, 94, 5264–5272.
- Störmer, C. (1955), *The Polar Aurora*, Oxford Univ. Press, Oxford, U. K.
- Swann, W. F. G. (1933), Application of Liouville's theorem to electron orbits in the Earth's magnetic field, *Phys. Rev.*, 44, 224–227.
- Tsyganenko, N. A. (1995), Modeling the Earth's magnetospheric magnetic field confined within a realistic magnetopause, *J. Geophys. Res.*, 100, 5599–5612.

- Tsyganenko, N. A. (1996), Effects of the solar wind conditions on the global magnetospheric configuration as deduced from data-based field models, *Eur. Space Agency Spec. Publ., ESA SP-389*, 181–185.
- Wilson, J. W., J. Miller, A. Konradi, and F. A. Cucinotta (1997), Shielding strategies for human space exploration, *NASA Conf. Publ.*, 3360, 435–446.
- Winglee, R. M., and E. M. Harnett (2007), Radiation mitigation at the Moon by the terrestrial magnetosphere, *Geophys. Res. Lett.*, 34, L21103, doi:10.1029/2007GL030507.
- 
- C.-L. Huang and H. E. Spence, Center for Space Physics, Boston University, 725 Commonwealth Avenue, Boston, MA 02215, USA. (hcl@bu.edu)
- B. T. Kress, Department of Physics and Astronomy, Dartmouth College, 6127 Wilder Laboratory, Hanover, NH 03755, USA.